

## Mechanistic Aspects of the Oxidative and Reductive Fragmentation of *N*-Nitrosoamines: A New Method for Generating Nitrenium Cations, Amide Anions, and Aminyl Radicals

Krzysztof Piech,<sup>†</sup> Thomas Bally,<sup>\*,†</sup> Adam Sikora,<sup>§</sup> and Andrzej Marcinek<sup>\*,§</sup>

Contribution from the Department of Chemistry, University of Fribourg, CH-1700 Fribourg, Switzerland, and Institute of Applied Radiation Chemistry, Technical University of Lodz, 90-924 Lodz, Poland

E-mail: Thomas.Bally@unifr.ch; Marcinek@p.lodz.pl

**Abstract:** A new method for investigating the mechanisms of nitric oxide release from NO donors under oxidative and reductive conditions is presented. Based on the fragmentation of *N*-nitrosoamines, it allows generation and spectroscopic characterization of nitrenium cations, amide anions, and aminyl radicals. X-irradiation of *N*-nitroso-*N,N*-diphenylamine **1** in Ar matrices at 10 K is found to yield the corresponding radical ions, which apparently undergo spontaneous loss of NO<sup>•</sup> under the conditions of this experiment (**1**<sup>•+</sup> seems to survive partially intact, but not **1**<sup>•-</sup>). One-electron reduction or oxidation of **1** is observed upon doping of the Ar matrix with DABCO, an efficient hole scavenger, or CH<sub>2</sub>Cl<sub>2</sub>, an electron scavenger, respectively. The resulting diphenylnitrenium cation, **2**<sup>+</sup>, and the diphenylamide anion, **2**<sup>-</sup>, were characterized by their full UV–vis and mid-IR spectra. The best spectra of **2**<sup>+</sup> and **2**<sup>-</sup> were obtained if **1** was homolytically photodissociated to diphenylaminyl radical **2**<sup>•</sup> and NO<sup>•</sup> prior to ionization. **2**<sup>+</sup> and **2**<sup>-</sup> are bleached on irradiation at <340 nm to form **2**<sup>•</sup> or, in part, **1**. DFT and CCSD quantum chemical calculations predict that the dissociation of **1**<sup>•+</sup> and **1**<sup>•-</sup> is slightly endothermic, a tendency which is partially reversed if one allows for complexation of the resulting **2**<sup>+</sup> (and, presumably, **2**<sup>-</sup>) with NO<sup>•</sup>. The method described in this work should prove generally applicable to the generation and study of nitrenium cations and amide anions R<sub>2</sub>N<sup>+/-</sup> under matrix and ambient conditions (i.e., in solution).

### 1. Introduction

Nitric oxide, due to its important physiological functions as a mediator in vascular muscle relaxation and a messenger in cellular signaling, has received enormous attention after the initial reports of its biological activity. Interest has also focused on nitric oxide synthase inhibitors and NO donors as potential therapeutic products.<sup>1,2</sup> Among the latter, *S*-nitrosothiols are considered to be ubiquitous biological NO donors, but, in spite of their importance as sources of NO, the mechanism of their decomposition has remained largely unexplained. Under physiological conditions, *S*-nitrosothiols are found to undergo homolytic fragmentation to yield NO<sup>•</sup>, but also heterolytic fragmentation to yield NO<sup>+</sup> and NO<sup>-</sup>. Reductive and oxidative decomposition has been proposed as more rapid and effective than S–NO bond homolysis.<sup>3–8</sup>

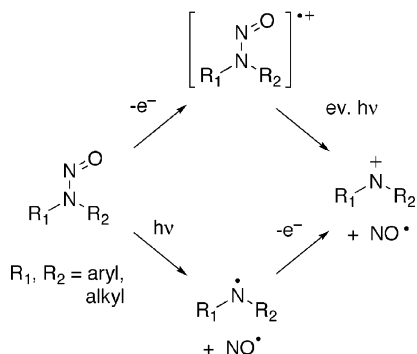
On the other hand, *N*-nitrosoamines, another class of potent NO donors showing vasorelaxant activity,<sup>9,10</sup> are generally considered as carcinogens.<sup>2</sup> For *N*-nitroso-*N,N*-diphenylamine, the genotoxicity and carcinogenicity studies remain, however, largely inconclusive, and the mechanism of the appearance of mutagenicity is unknown<sup>11,12</sup> (a cytochrome P-450-dependent, reductive denitrosation mechanism for the induction of DNA single strand breaks has been suggested<sup>13</sup>). In this paper, we report experimental and theoretical studies on the homolytic or heterolytic fragmentation of *N*-nitroso-*N,N*-diphenylamine under oxidative and reductive conditions. The mechanistic details of the investigated reactions may be directly related to the role of *N*-nitrosoamines as NO donors in biological processes. Moreover, the mechanistic aspects related to the homolytic or heterolytic cleavage of the N–NO bond are similar to those of the S–NO bond.<sup>2,14</sup>

<sup>†</sup> University of Fribourg.

<sup>§</sup> Technical University of Lodz.

- (1) Janero, D. R. *Free Radical Biol. Med.* **2000**, 28, 1495.
- (2) Wang, P. G.; Xian, M.; Tang, X.; Wu, X.; Wen, Z.; Cai, T.; Janczuk, A. *J. Chem. Rev.* **2002**, 102, 1091.
- (3) Williams, D. L. H. *Acc. Chem. Res.* **1999**, 32, 869.
- (4) Grossi, L.; Montevecchi, P. C.; Strazzari, S. *J. Am. Chem. Soc.* **2001**, 123, 4853.
- (5) Grossi, L.; Montevecchi, P. C. *Chem. Eur. J.* **2002**, 8, 380.
- (6) Stämmler, J. S.; Toone, E. J. *Curr. Opin. Chem. Biol.* **2002**, 6, 779.
- (7) Zhao, Y. L.; McCarren, P. R.; Houk, K. N.; Choi, B. Y.; Toone, E. J. *J. Am. Chem. Soc.* **2005**, 127, 10917.
- (8) Manoj, V. M.; Mohan, H.; Aravind, U. K.; Aravindakumar, C. T. *Free Radical Biol. Med.* **2006**, 41, 1240.
- (9) Lippton, H. L.; Gruetter, C. A.; Ignarro, L. J.; Meyer, R. L.; Kadowitz, P. J. *Can. J. Physiol. Pharmacol.* **1982**, 60, 68.
- (10) DeRubertis, F. R.; Craven, P. A. *Science* **1976**, 193, 897.
- (11) Negishi, T.; Shiotani, T.; Fujikawa, K.; Hayatsu, H. *Mutat. Res.* **1991**, 252, 119.
- (12) Zielenska, M.; Guttenplan, J. B. *Mutat. Res.* **1988**, 202, 269.
- (13) Appel, K. E.; Gorsdorf, S.; Scheper, T.; Bauszus, M.; Hildebrandt, A. G. *Arch. Toxicol.* **1987**, 60, 204.
- (14) Zhu, X.-Q.; He, J.-Q.; Xian, M.; Lu, J.; Cheng, J.-P. *J. Org. Chem.* **2000**, 65, 6729.

**Scheme 1.** Strategies To Obtain Nitrenium Cations from *N*-Nitrosoamines



As a wide range of alkyl- or aryl-substituted *N*-nitrosoamines are stable and commercially available, we developed a strategy, reported in this paper, which allows in principle to study the mechanistic aspects of the NO-releasing process under conditions where the transient products which occur in the investigated reactions persist sufficiently long to be probed and characterized by conventional spectroscopic means. One type of such transient species expected on oxidative fragmentation of nitrosoamines are nitrenium cations (reactive intermediates that contain a divalent, positively charged nitrogen atom; see Scheme 1).<sup>15,16</sup> Apart from their being hypovalent species with a peculiar electronic structure,<sup>15</sup> the biological role of aryl nitrenium cations in carcinogenesis provides a strong incentive for studying their structure and reactivity.

In kinetic studies, nitrenium cations are usually generated by photolysis of ionic precursors (anthralinium cations,<sup>17</sup> *N*-aminopyridinium cations<sup>18</sup>), by photoinduced N–X heterolysis (X = Cl, OSO<sub>3</sub>, OAc),<sup>19</sup> or by protonation of photogenerated nitrenes.<sup>20</sup> These techniques have allowed mainly the groups of Falvey<sup>21,22</sup> and McClelland<sup>23,24</sup> and some others to characterize many aryl nitrenium cations by transient UV/vis (and recently also by transient IR<sup>25</sup> and Raman<sup>26</sup>) spectroscopy and to determine the kinetics of their reactions with various electron-rich arenes<sup>27</sup> and with guanine bases.<sup>24,28</sup> However, most of the above schemes suffer from one or the other limitation with regard to the types of nitrenium cations that can be generated, and they invariably involve the presence of counterions which increase the polarity of the surrounding medium and may perturb thus some inherent properties of the nitrenium cations. Finally, these species appear only as transient intermediates in the above studies, which precludes their full spectroscopic characterization.

We chose *N*-nitroso-*N,N*-diphenylamine as a first target because, in contrast to the sparse spectral features of small species like NO• and its ions, arylaminyl radicals and nitrenium/amide ions can be unambiguously characterized and used as markers of the possible pathways of nitrosoamine fragmentation. Second, the transient UV/vis and a part of the transient IR spectrum of the diphenylnitrenium cation are known from previous solution studies.<sup>29,30</sup> Before looking into the fate of the nitrosoamine on ionization (which was expected to produce the diphenylaminyl radical as a secondary product), we studied its photolysis as a neutral species.

## 2. Methods

*N*-Nitroso-*N,N*-diphenylamine **1** (Aldrich, >97% pure) was purified by sublimation and subsequent recrystallization from ethanol to yield bright yellow crystals which were placed in a U-tube attached to the inlet system of the cryostat and carefully degassed. After that, a stream of a 10:1 Ar/N<sub>2</sub> mixture, doped with about 1% of an electron or hole scavenger (see below), was led through the U-tube at room temperature. Thereby, deposition of a suitable amount of the nitrosoamine **1** on the CsI window, held at 20 K, occurred. Ionization was effected by X-irradiation of the resulting matrix,<sup>31</sup> which leads predominantly to the ionization of Ar. The resulting holes and electrons propagate through the matrix until the holes meet a species with a lower oxidation potential than Ar, and the electrons one with a higher electron affinity, whereupon both charges get trapped.

If radical cations are targeted, the matrix is doped with CH<sub>2</sub>Cl<sub>2</sub>, which acts as an efficient electron scavenger,<sup>31</sup> at least until a certain concentration of radical cations has built up. After about 10–15% of the neutral precursor has been converted to radical cations, those begin to compete effectively with CH<sub>2</sub>Cl<sub>2</sub> for liberated electrons, and the amount of charged species in the matrix begins to level off. Under our experimental conditions, this asymptotic limit is usually reached after about 1.5 h of X-irradiation.

If radical anions are to be formed, the matrix is doped with 1,4-diazabicyclo[2.2.2]octane (DABCO), an excellent hole scavenger which has the advantage that its radical cation has an unobtrusive UV/vis spectrum (a weak, broad band peaking at 450 nm) and a very simple IR spectrum consisting essentially of a single, intense peak at 713.5 cm<sup>-1</sup> (see Supporting Information).

Electronic absorption (Perkin-Elmer Lambda 900) and infrared spectra (Bomem DA3) were measured before and after ionization or subsequent photolyses and are presented as difference spectra. Photolyses were effected with a high-pressure Hg/Xe arc through appropriate interference and/or cutoff filters, or with a low-pressure Hg lamp (254 nm).

The geometries of all species were optimized by the B3LYP density functional method<sup>32,33</sup> using the 6-31G\* basis set. All stationary points were characterized by calculating second derivatives of the energy. These served also to model IR spectra and the statistical thermodynamic corrections needed to calculate relative enthalpies or free energies. Excited-state calculations were carried out on the basis of time-dependent response theory, also with the B3LYP density functional method (the so-called TD-DFT method)<sup>34</sup> as implemented in the Gaussian suite of programs<sup>35</sup> which was used in all the calculations.<sup>36</sup>

- (15) Falvey, D. E. Nitrenium Ions. In *Reactive Intermediate Chemistry*; Moss, R. A., Platz, M. S., Jones, M., Eds.; John Wiley & Sons: Hoboken, NJ, 2004; p 593.
- (16) Novak, M.; Xu, L.; Wolf, R. A. *J. Am. Chem. Soc.* **1998**, *120*, 1643.
- (17) Haley, N. F. *J. Org. Chem.* **1977**, *42*, 3929.
- (18) Takeuchi, H.; Koyoma, K. *J. Chem. Soc., Perkin Trans.* **1988**, *1*, 2277.
- (19) Davidse, P. A.; Kahley, M. J.; McClelland, R. A.; Novak, M. *J. Am. Chem. Soc.* **1994**, *116*, 4513.
- (20) McClelland, R. A.; Davidse, P. A.; Hadzialic, G. *J. Am. Chem. Soc.* **1996**, *118*, 4794.
- (21) Robbins, R. J.; Yang, L. L.-N.; Anderson, G. B.; Falvey, D. E. *J. Am. Chem. Soc.* **1995**, *117*, 6544.
- (22) Robbins, R. J.; Laman, D. M.; Falvey, D. E. *J. Am. Chem. Soc.* **1996**, *118*, 8127.
- (23) McClelland, R. A.; Davidse, P. A.; Hadzialic, G. *J. Am. Chem. Soc.* **1995**, *117*, 4173.
- (24) McClelland, R. A.; Gadosy, T. A.; Ren, D. *Can. J. Chem.* **1998**, *76*, 1327.
- (25) Srivastava, S.; Ruane, P. H.; Toscano, J. P.; Sullivan, M. B.; Cramer, C. J.; Chiapperino, D.; Reed, E. C.; Falvey, D. E. *J. Am. Chem. Soc.* **2000**, *122*, 8271.
- (26) Zhu, P.; Ong, S. Y.; Chan, P. Y.; Poon, Y. F.; Leung, K. H.; Phillips, D. L. *Chem. Eur. J.* **2001**, *7*, 4928.
- (27) McIlroy, S.; Falvey, D. E. *J. Am. Chem. Soc.* **2001**, *123*, 11329.
- (28) Novak, M.; Kennedy, S. A. *J. Am. Chem. Soc.* **1995**, *117*, 574.

- (29) Moran, R. J.; Falvey, D. E. *J. Am. Chem. Soc.* **1996**, *118*, 8965.
- (30) Srivastava, S.; Toscano, J. P.; Moran, R. J.; Falvey, D. E. *J. Am. Chem. Soc.* **1997**, *119*, 11552.
- (31) Bally, T. Matrix Isolation. In *Reactive Intermediate Chemistry*; Moss, R. A., Platz, M. S., Jones, M., Eds.; John Wiley & Sons: Hoboken, NJ, 2004; p 820.
- (32) Becke, A. D. *J. Chem. Phys.* **1992**, *97*, 9173.
- (33) Lee, C.; Yang, W.; Parr, R. G. *Phys. Rev. B* **1988**, *37*, 785.
- (34) Casida, M. E. Time-Dependent Density Functional Response Theory for Molecules. In *Recent Advances in Density Functional Methods, Part I*; Chong, D. P., Ed.; World Scientific: Singapore, 1995; p 155.

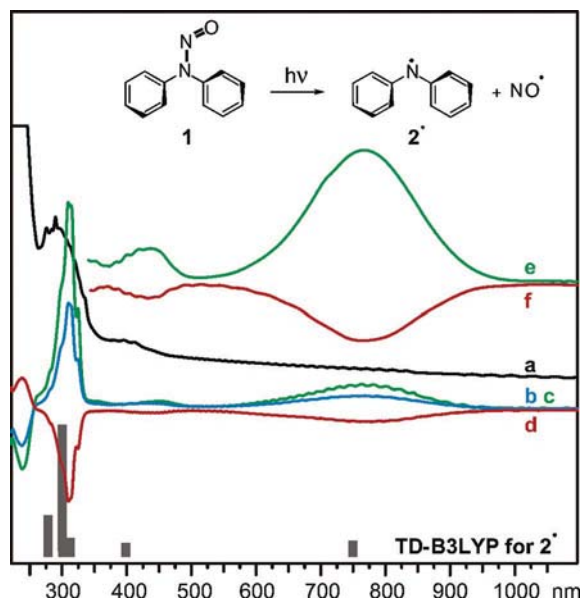


**Figure 1.** Difference spectra for the photodissociation of **1** to give **2\*** and  $\text{NO}^*$  in an Ar matrix at 10 K (spectra a–d are from an experiment with a low concentration and spectra e and f from one with a higher concentration of **1**).

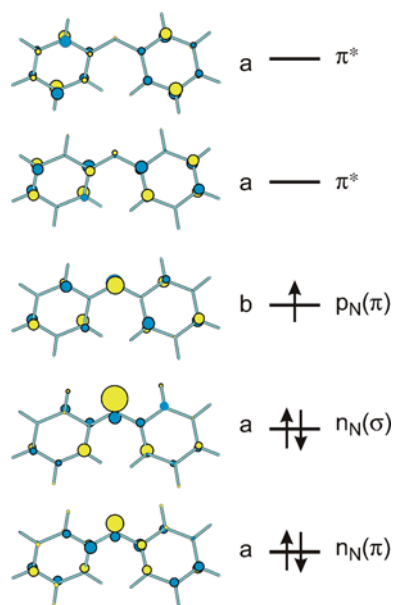


**Figure 2.** MOs of **2** involved in the electronic transitions of **2\***,  $2^+$ , and  $2^-$  (electronic ground configuration for **2\*** is shown). Note that some occupied  $\pi$  MOs lie between the two  $n_N$  MOs.

### 3. Results and Discussion

**3.1. Homolytic Fragmentation of *N*-Nitroso-*N,N*-diphenylamine **1**.** The homolytic bond dissociation energies (BDEs) for various substituted *N*-nitroso arylamines are in the range of 20–30 kcal/mol, lower than those of *N*-carbonyl nitroso compounds<sup>14</sup> but similar to the values for the S–NO bonds in aromatic and alkyl nitrosothiols.<sup>7,14,37</sup> Although N–NO bonds are over 60 kcal/mol weaker than the corresponding N–H bonds, their homolytic cleavage still requires substantial activa-

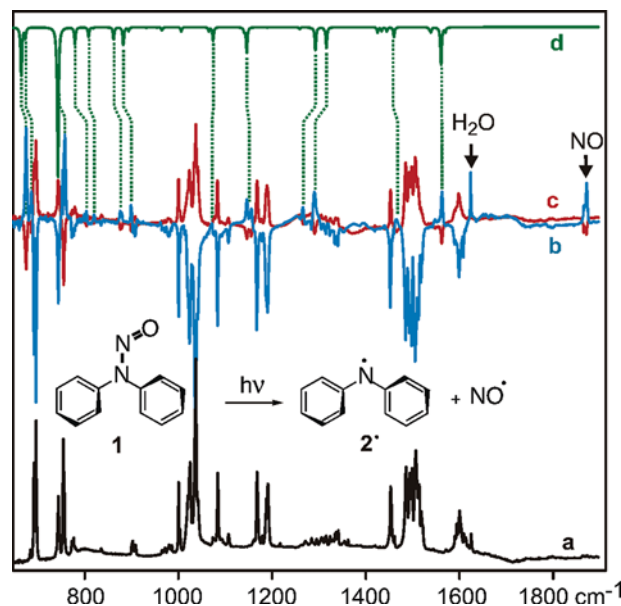


**Figure 3.** Changes in the IR spectra upon photodissociation of **1** (b) and its re-formation by NIR irradiation (c) in an Ar matrix. (a) Absolute spectrum of **1**. Top: IR spectrum of **2\*** calculated by B3LYP/6-31G\*.

tion which can be delivered, for example, through photoexcitation of *N*-nitrosoamines.

Although it barely absorbs at this wavelength, nitrosamine **1** already undergoes slow photodecomposition at 400 nm (blue difference spectrum b in Figure 1), but **1** is photolyzed more efficiently by irradiation at 254 nm (green difference spectrum c) to form the diphenylaminyl radical, **2\***.<sup>38</sup> This compound reveals itself by its broad band peaking at 770 nm, which is accompanied by a weaker feature at 400–500 nm.<sup>39–41</sup> In addition to these previously recorded bands, we recorded an intense, structured peak at 310 nm.

TD-B3LYP predictions for the spectrum of **2\*** (black bars at the bottom of Figure 1 and Table 1 in the Supporting Information) are in excellent accord with the observed spectrum. According to these calculations, the broad visible band is mainly due to electron excitation for the  $n_N(\sigma)$  molecular orbital (MO) to the  $p_N(\pi)$  singly occupied molecular orbital (SOMO), while the smaller band peaking at 440 nm involves promotion from the lower-lying  $n_N(\pi)$  MO to the SOMO (see MOs in Figure 2). The UV band consists essentially of two excitations which involve positive and negative combinations of the electron promotions from the SOMO to the two  $\pi^*$  MOs in Figure 2.

On irradiation at >850 nm (or, more efficiently, at >515 nm), the spectrum of **2\*** is partially bleached (red spectra d and f in Figure 1). The IR spectra shown in Figure 3 reveal that the cleavage of **1** is actually photoreversible in Ar, in that the bands of **1** (black spectrum a) which are bleached on 400 or 254 nm photolysis (blue spectrum b) clearly reappear on >515 nm irradiation (red spectrum c), whereas the 1836  $\text{cm}^{-1}$  peak of the NO radical shows the inverse behavior. Apparently, **2\*** and

(35) Stratmann, R. E.; Scuseria, G. E.; Frisch, M. J. *J. Chem. Phys.* **1998**, *109*, 8218.  
(36) Frisch, M. J.; et al. *Gaussian 98*, Revision A7–A11; Gaussian Inc.: Pittsburgh, PA, 1998; *Gaussian 03*, Revision C01; Gaussian Inc.: Wallingford, CT, 2004 (for full citations, see Supporting Information).

(37) Lu, J.-M.; Wittbrodt, J. M.; Wang, K.; Wen, Z.; Schlegel, H. B.; Wang, P. G.; Cheng, J.-P. *J. Am. Chem. Soc.* **2001**, *123*, 2903.  
(38) Wagner, B. D.; Ruel, G.; Luszyk, J. *J. Am. Chem. Soc.* **1996**, *118*, 13.  
(39) Shida, T.; Kira, A. *J. Phys. Chem.* **1969**, *73*, 4315.  
(40) Levya, E.; Platz, M. S.; Niu, B.; Wirz, J. *J. Phys. Chem.* **1987**, *91*, 2293.  
(41) DiLabio, G. A.; Litwinienko, G.; Lin, S.; Pratt, D. A.; Ingold, K. U. *J. Phys. Chem. A* **2002**, *106*, 11719.



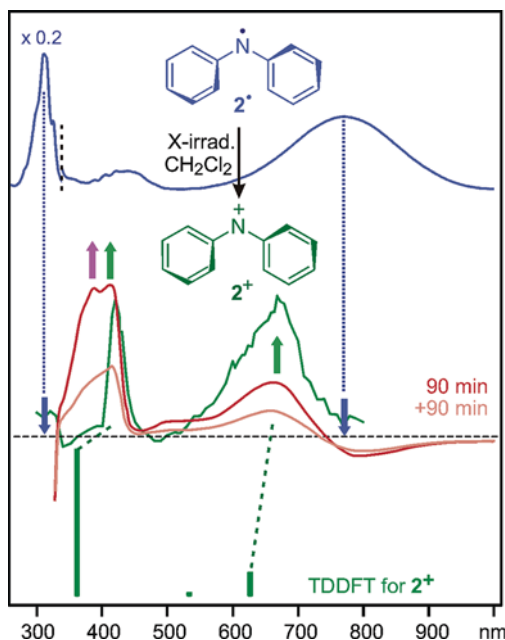


**Figure 4.** Spectral changes on X-irradiation of a  $\text{CH}_2\text{Cl}_2$ -doped Ar matrix containing aminyl radical  $2^\bullet$  (blue spectrum) for 90 min (red spectrum) and then another 90 min (orange spectrum). The green trace is a copy of the spectrum of  $2^+$  obtained by Moran and Falvey by flash photolysis of the *N*-diphenylaminopyridinium tetrafluoroborate in  $\text{CH}_3\text{CN}/\text{CF}_3\text{COOH}$ .<sup>29</sup> Bottom: TD-B3LYP predictions of the electronic transitions of  $2^+$  (for details, see Supporting Information).

$\text{NO}^\bullet$ , which survive next to each other in the thermalized matrix, re-combine on excitation of  $2^\bullet$ , perhaps as a consequence of a local annealing of the matrix.

In general, ca. 50% of **1** can be photodecomposed by irradiating for 1–2 h at 254 nm (up to 75% on prolonged irradiation). Only about half of the formed  $2^\bullet$  is, however, reconverted to **1** upon NIR bleaching, because apparently some of the  $\text{NO}$  radicals have escaped the matrix cavity and cannot be recaptured by  $2^\bullet$ . We believe that the latter process, which is probably activationless in solution, involves local annealing of the matrix by excited  $2^\bullet$  trying to dissipate its excess energy.

In the above experiments,  $2^\bullet$  revealed also its complete IR spectrum, which has not been reported to date. This spectrum turns out to be in very good accord with the B3LYP/6-31G\* prediction (green trace d in Figure 2). Due to extensive mode mixing, none of the IR transitions can, however, be associated unambiguously with individual valence deformations, such as the symmetric and antisymmetric C–N stretching mode.

**3.2. Radiolysis of the Diphenylaminyl Radical  $2^\bullet$ .** The above-described experiments did not yield any evidence for heterolysis of **1** on 254 nm photolysis in Ar matrices. As a good yield of  $2^\bullet$  can be obtained by photolysis of **1**, we decided to subject the resulting samples directly to ionization by radiolysis, to obtain the diphenylnitrenium cation,  $2^+$ . On exposing a  $\text{CH}_2\text{Cl}_2$ -doped Ar matrix containing ca. 50% of **1** and  $2^\bullet$  to 90 min of X-irradiation two times, the UV–vis spectral changes documented in Figure 4 were observed.

While the bands of  $2^\bullet$  decrease, new bands arise which peak at 665 (broad), ca. 500 (shoulder), 415, and 386 nm (both sharp and intense). However, the difference spectrum obtained on the second 90 min irradiation indicates that not all these bands belong to the same species. In particular, the 386 nm peak grows much less in this second radiolysis than the others. This hunch

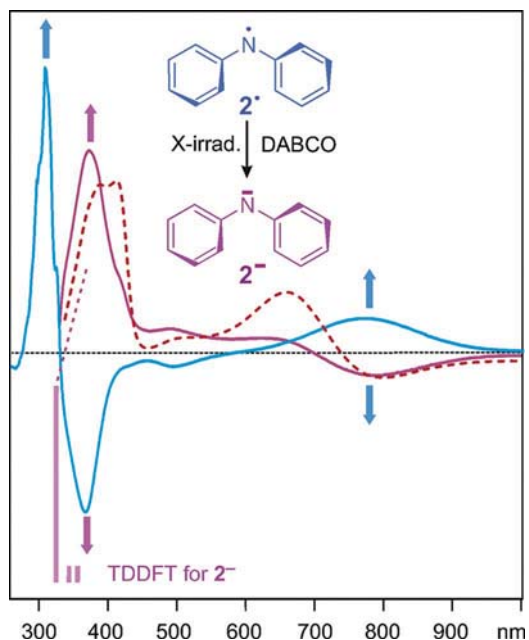


**Figure 5.** Spectral changes upon X-irradiation of a DABCO-doped Ar matrix containing aminyl radical  $2^\bullet$  for 90 min (purple spectrum) and after subsequent bleaching at 313 nm (blue spectrum). The bands of  $2^\bullet$  are marked with blue arrows, those of the amide anion  $2^-$  with purple arrows. Red dotted line, red spectrum from Figure 4. Bottom: TD-B3LYP prediction of the electronic transitions of  $2^-$  (for details, see Supporting Information).

is confirmed by comparing the present spectra to that of  $2^+$ , measured previously by Moran and Falvey,<sup>29</sup> which corresponds to the green trace in Figure 4. Indeed, the bands at 665 and 415 nm in that spectrum coincide with the present ones, whereas that at 386 nm is absent from the spectrum of Moran and Falvey. The pattern of bands assigned to  $2^+$  correlate also reasonably well with that from TD-DFT predictions for this species, although quantitative agreement is not as good as for  $2^\bullet$ .

In terms of the MOs in Figure 2, the two bands in the spectrum of  $2^+$  are caused by positive and negative combinations of electron promotions from  $n_N(\sigma)$  and  $n_N(\pi)$  to the (now empty)  $p_N/\pi$  MO (cf. Table 2 in the Supporting Information).

In view of our recent discovery that species with a sufficiently high electron affinity may compete successfully with  $\text{CH}_2\text{Cl}_2$  for the electrons liberated in the X-irradiation of Ar,<sup>42</sup> we decided to examine whether  $2^\bullet$  had perhaps also undergone reduction in this process. If indeed the amide anion  $2^-$  was formed, its yield would be expected to increase if DABCO is added as a hole scavenger. The UV/vis spectra resulting from this experiment are shown in Figure 5.

From these spectra we determine that  $2^\bullet$  is again consumed in the process of X-irradiation (its typical broad 770 nm band decreases in the purple difference spectrum), while a new band peaking at 386 nm arises next to a shoulder at 415 nm, which is probably due to some  $2^+$  that is formed even under these conditions (there is also an indication of the broad 665 nm band of this compound in the difference spectrum), and a bump around 500 nm.

Upon photolysis at 313 nm, the spectrum that was formed on X-irradiation is bleached (blue difference spectrum), whereby the absorptions of  $2^\bullet$  are re-formed (blue arrows). The mech-

(42) Czerwinska, M.; Sikora, A.; Szajerski, P.; Zielonka, J.; Adamus, J.; Marcinek, A.; Piech, K.; Bednarek, P.; Bally, T. *J. Org. Chem.* **2006**, *71*, 5312.

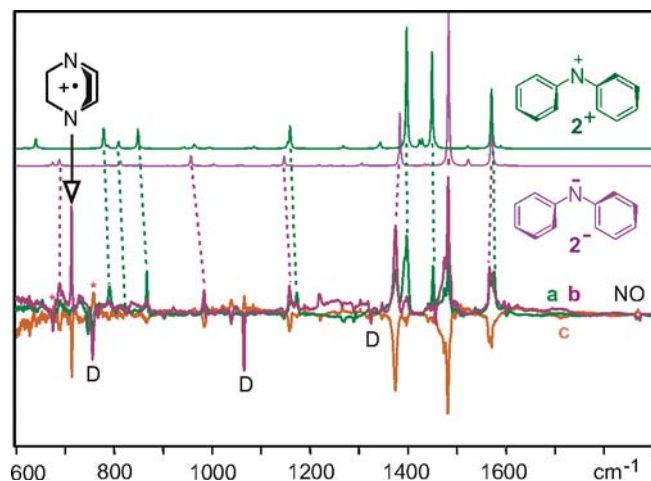


**Figure 6.** IR difference spectra for the X-radiolysis of an Ar matrix containing **1** and **2•** + **NO•** in a ca. 1:1 ratio in the presence of  $\text{CH}_2\text{Cl}_2$  (green spectrum, a) or DABCO (purple spectrum, b). The orange spectrum, c, corresponds to the 313 nm bleaching of the sample giving spectrum b (the peaks labeled D are due to DABCO, those marked with red asterisks are due to **2•**). Top: IR spectra of **2⁺** (green) and **2⁻** (purple) calculated by B3LYP/6-311G(2d,p).

anism of this process probably involves electron photodetachment (and therefore neutralization) from the anion and ensuing reneutralization of the cations present in the matrix (mainly  $\text{DABCO}^{•+}$  and some **2⁺**).

The UV band of **2⁻** has previously been observed after dissociative electron attachment to *N,N*-diphenyl- and tetraphenylhydrazine ( $\lambda_{\text{max}} = 380 \text{ nm}$ )<sup>39</sup> and after deprotonation of diphenylamine ( $\lambda_{\text{max}} = 373 \text{ nm}$ ).<sup>43</sup> Our present observations are in good accord with these reports. TD-DFT calculations predict one intense and two small UV transitions for the amide anion **2⁻**, all of which are probably hidden in the intense 386 nm band. The transitions are positive and negative combinations of the electron promotions from the  $p_N/\pi$  highest occupied molecular orbital (HOMO; doubly occupied in **2⁻**) to the two  $\pi^*$  MOs shown in Figure 2.

In Figure 6, the IR spectra for the above-described processes are juxtaposed. By comparing the green and purple spectra, it is clearly seen that two compounds are formed, in different proportions, on X-irradiation of matrices doped with the electron scavenger,  $\text{CH}_2\text{Cl}_2$ , or the hole scavenger, DABCO, and that in the latter case both species are bleached upon photolysis at 313 nm (in addition to the radical cation of DABCO).

The IR spectrum of **2⁺** between 1200 and 1700  $\text{cm}^{-1}$  has been measured previously by time-resolved spectroscopy in the laboratories of Toscano et al.,<sup>30</sup> and the three strong peaks at 1392, 1442, and 1568  $\text{cm}^{-1}$  that had been assigned to **2⁺** are found with the same intensity ratio in our present experiments (at 1397, 1450, and 1575  $\text{cm}^{-1}$ ). With the aid of the calculated spectra of **2⁺** and **2⁻**, it is easy to assign these and most of the other peaks in the IR spectra (cf. dashed lines) to these two species.

In sum, we have been able to convert the aminyl radical **2•**, pre-formed by photolysis of **1** in an Ar matrix, into the nitrenium cation **2⁺** and the amide anion **2⁻** by X-irradiation of that Ar matrix. Their distinctive spectral features in the UV/vis and IR leaves no doubt that photochemical decomposition of *N*-nitroso-*N,N*-diphenylamine in Ar occurs exclusively by homolysis.

**3.3. Ionization of *N*-Nitroso-*N,N*-diphenylamine **1**.** As the homolytic fragmentation of *N*-nitrosoamines, similar to the

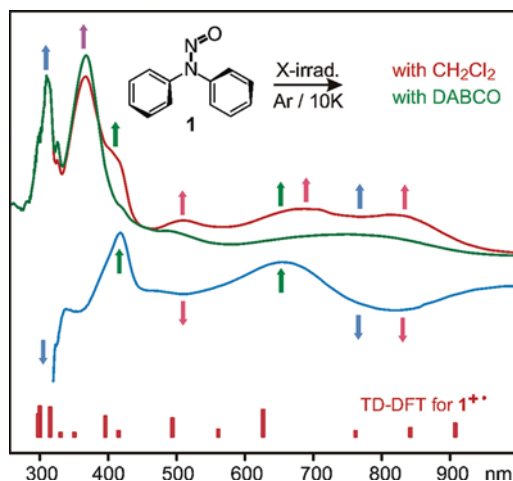


**Figure 7.** Spectral changes on X-irradiation of an Ar matrix containing **1** when it is doped with DABCO (green spectrum) or  $\text{CH}_2\text{Cl}_2$  (red spectrum). The blue spectrum shows the spectral changes on bleaching the sample giving the red spectrum at  $>850 \text{ nm}$ . The arrows indicate the positions of the bands of **2•** (blue), **2⁺** (green), and **2⁻** (purple). Bottom: TD-B3LYP prediction of the electronic spectrum of the radical cation of **1** (for details, see Supporting Information).

decomposition of *S*-nitrosothiols, is an endothermic process, we explored other possibilities of N–NO bond cleavage. As redox reactions are known to have a strong influence on the strength of bonds that are cleaved in chemical and biological reactions, we investigated the homolytic vs heterolytic fragmentation also under reductive and oxidative conditions.

On exposing an Ar matrix containing roughly equimolar amounts of **1** and DABCO to 90 min of X-irradiation, the green spectrum in Figure 7 is obtained. It clearly shows the formation of **2⁻** (purple arrow) and **2•** (blue arrows). Apart from the omnipresent 500 nm shoulder (which we have not been able to assign so far), there is no indication for the formation of any other species, also in the IR spectra (not shown). Thus, the fragmentation of **1•⁻** is apparently spontaneous under the present conditions. On NIR irradiation, the bands of **2•** are bleached, while the intense UV band of **2⁻** is not affected, whereas 313 nm photolysis leads to the disappearance of the latter and the formation of **2•**.

If the matrix is doped with  $\text{CH}_2\text{Cl}_2$  instead, the much more complex red spectrum shown in Figure 7 arises. In that spectrum, we can again discern the formation of **2⁻**, **2•**, and much more **2⁺** than in the experiment with DABCO. However, in contrast to that experiment, the difference spectrum clearly indicates the presence of at least one additional species, the bands of which are indicated by red arrows in Figure 7. Upon irradiation at  $>850 \text{ nm}$  (blue spectrum), these bands are bleached, along with those of **2•**, which is also photosensitive at this wavelength. Concomitantly, the bands of **2⁺** rise in intensity (see green arrows).

The IR spectra for these experiments confirmed the formation of **2⁻**, **2•**, and **2⁺** (and their bleaching, where this is possible), but they failed to reveal any useful information about the identity of the additional new compound observed in the experiment with  $\text{CH}_2\text{Cl}_2$ . Thus, we are left to speculate that it is probably the radical cation of **1**. A TD-B3LYP calculation of the optical spectrum of **1•⁺** gave the result shown graphically at the bottom

(43) Shashin, S. S.; Emanuel, O. N.; Skibida, I. P. *Russ. Chem. Bull.* **1994**, 43, 1646.

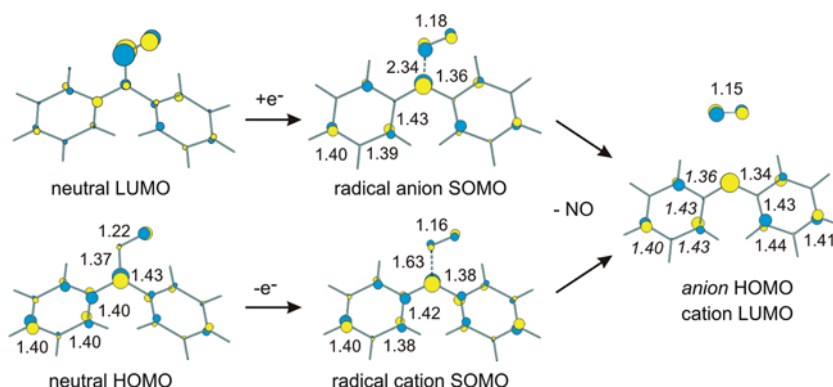


**Figure 8.** Change in bond lengths and frontier MOs on ionization of **1** and subsequent loss of  $NO^*$  from the resulting radical ions,  $1^{*+}$  and  $1^{*-}$  (SOMO = singly occupied MO), to yield the closed-shell ions,  $2^+$  and  $2^-$ , respectively, as calculated by the B3LYP/6-31G\* method (see Supporting Information for full geometries).

of Figure 7, which indicates that  $1^{*+}$  has many electronic transitions in the range where we can observe spectra. Although this prediction cannot be taken as conclusive evidence for the presence of  $1^{*+}$ , it is not in contradiction with a corresponding assignment of the newly observed bands (red arrows in Figure 7).

Thus, it seems that  $1^{*+}$  — in contrast to  $1^{*-}$ , for which we have no evidence whatsoever — survives at least partially after being formed by charge transfer from  $Ar^{*+}$ , a process that leaves the incipient cation with substantial excess energy.<sup>31</sup> On NIR photolysis,  $1^{*+}$  is cleaved to yield  $2^+ + NO^*$ . Both  $2^+$  and  $2^-$  are neutralized in part to  $2^*$  by the electrons and holes that are continually generated during the X-irradiation of Ar. Of course, once  $2^*$  is formed, the holes and electrons will attach to it to re-form  $2^+$  and  $2^-$ , in a proportion that depends on the presence of the electron or hole scavenger.

The processes observed on X-irradiation of Ar matrices containing **1** are summarized in Scheme 2. An interesting corollary of these experiments is that there is no indication for the ionization of **1** in the presence of  $2^*$ . Apparently, the lower ionization potential of the latter species causes it to preferentially scavenge the holes that are formed on X-irradiation of Ar.

To gain insight into the thermochemistry and the mechanisms of the above processes, we carried out some quantum chemical calculations that are described in the following section.

**3.4. Quantum Chemical Calculations.** Figure 8 shows how the frontier MOs and the bond lengths change as **1** is ionized and as the resulting radical ions lose  $NO^*$  to form  $2^+$  and  $2^-$ , respectively. While removal of an electron is from the HOMO of **1**, which is slightly bonding along the N–N bond, addition of an electron is to the LUMO of **1**, which is N–N antibonding. Thus, it comes as no surprise that the N–N bond lengthens considerably in the course of both processes, to the point where  $1^{*-}$  must be regarded as a complex between  $2^-$  and  $NO^*$ . Concomitantly, the N–O bond length shrinks, almost to the value of 1.15 Å it has in the free  $NO$  radical.

Upon full dissociation, which, according to B3LYP/6-31G\* calculations, is endothermic by ca. 8 kcal/mol in both radical ions (cf. Table 1), the bond length pattern in the resulting species is indicative of the iminocyclohexadienyl structure that has been noted previously for  $2^+$ ,<sup>30,44</sup> and which expresses itself particular in the very short C–N bonds. The geometries of  $2^+$  and  $2^-$  are very similar (and to that of  $2^*$ , not shown), which is to be

**Table 1.** Relative Energies [ $\Delta H(0\text{ K})$ , in kcal/mol] of Different Species Discussed in This Work

	B3LYP/6-31G*	RCCSD/6-31G*
<i>N</i> -nitroso- <i>N,N</i> -diphenylamine <b>1</b>	(0)	(0)
$2^+ + NO^*$	23.5	26.3
radical cation $1^{*+}$	(0) <sup>a</sup>	(0) <sup>b</sup>
$2^+ + NO^*$ (free)	8.04 <sup>c</sup>	6.21 <sup>d</sup>
$2^+ \cdots NO^*$ (complex)	5.47	
radical anion $1^{*-}$	(0) <sup>e</sup>	(0) <sup>f</sup>
$2^- + NO^*$ (free)	7.99 <sup>g</sup>	4.52 <sup>h</sup>

<sup>a</sup> Ionization energy of **1**, 7.47 eV. <sup>b</sup> Ionization energy of **1**, 7.55 eV. <sup>c</sup> Ionization energy of  $2^+$ , 6.80 eV. <sup>d</sup> Ionization energy of  $2^*$ , 6.68 eV. <sup>e</sup> Gas-phase electron affinity of **1**, −0.81 eV. <sup>f</sup> Gas-phase electron affinity of **1**, −0.12 eV. <sup>g</sup> Gas-phase electron affinity of  $2^+$ , −1.48 eV. <sup>h</sup> Gas-phase electron affinity of  $2^*$ , −1.06 eV. More negative electron affinities denote more strongly bound electrons.

expected because the bond lengths should not depend on the occupation number of the essentially nonbonding MO that is depicted on the right in Figure 8 (0 in  $2^+$ , 1 in  $2^*$ , or 2 in  $2^-$ ).

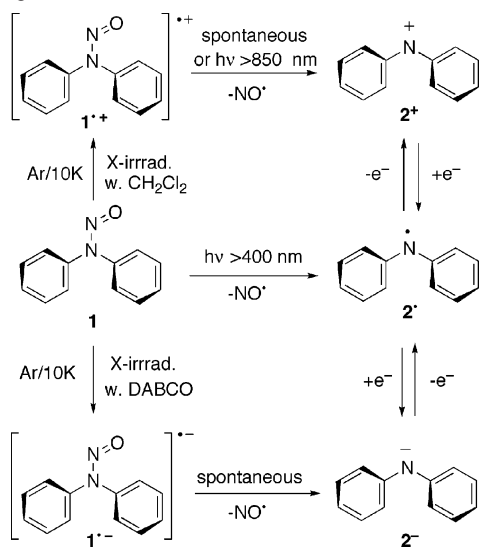
It is also interesting to follow the evolution of the frontier MOs along the reaction path: Whereas the HOMO and the LUMO of **1** are still quite distinct, the ensuing SOMOs of the two radical ions begin to resemble each other (apart from the presence or absence of nodes along the N–N bond or the C–C bonds, respectively). On loss of  $NO^*$ , the two MOs become nearly identical, so the wavefunctions change in a smooth way on lengthening the N–N bond in both species. Consequently, the re-combination of  $2^+$  and  $2^-$  with  $NO^*$  is (computationally) barrierless, and the question arises why the two ions persist in the presence of  $NO^*$  in Ar.

One reason could be that the B3LYP/6-31G\* predictions for the thermochemistry of the dissociation of  $1^{*+}$  and  $1^{*-}$  are wrong. Thus, we attempted to corroborate these predictions using a correlated wavefunction-based method, but this turned out to be difficult, because zero-order UHF wavefunctions for  $1^{*+}$  and  $2^*$  are so badly spin contaminated ( $\langle S^2 \rangle > 2$  in both cases) that it is impossible to rectify this by second-order perturbation theory, and therefore MP2 results become essentially meaningless. Thus, we resorted to coupled cluster calculations (where the perturbation series is basically taken to infinite order) based on a spin-restricted wavefunction (RCCSD), which gave the results listed in the third column of Table 1. Unfortunately, it proved impossible, with our current hardware, to estimate the contribution of triple excitations, i.e., do RCCSD-(T) calculations for the radical ions of **1**, and we are aware of

(44) Cramer, C. J.; Dulles, F. J.; Falvey, D. E. *J. Am. Chem. Soc.* **1994**, *116*, 9787.



**Scheme 2.** Processes Observed on X-Irradiation of Ar Matrices Containing **1**



the fact that the 6-31G\* basis set is not sufficiently flexible for coupled cluster calculations. However, the fact that the RCCSD predictions are in line with those from the DFT calculations (which are much less affected by problems of spin contamination,  $\langle S^2 \rangle < 0.78$ ) lends support to the notion that the dissociations of the radical ions of **1** are slightly endothermic.

In **1**<sup>•+</sup>, we explored also the possibility of re-complexing the cation, **2**<sup>+</sup>, with NO•. Of course, if the N end of NO• is brought into proximity of the nitrenium N atom, the two species collapse to re-form **1**<sup>•+</sup>. However, we found that the NO• also liked to enter into a loose complex with one of the benzene rings of **2**<sup>+</sup>, and the most stable of these complexes turned out to be bound by ca. 2.5 kcal/mol relative to **2**<sup>+</sup> + free NO• and stable with regard to spontaneous collapse to **1**<sup>•+</sup>.

The fact that the dissociation of the radical ions is slightly endothermic (although it is exergonic in the gas phase, mainly due to the gain in translational entropy which, however, cannot be realized in a matrix) is not a problem because the required activation can easily be provided by the excess energy that is imparted onto the incipient radical ions (or upon subsequent photoexcitation of **1**<sup>•+</sup>). Due to local annealing of the matrix by this excess energy, some of the NO radicals will escape the matrix cavity containing **2**<sup>+</sup> or **2**<sup>-</sup> and thus will not be able to re-combine with these ions. Others may remain trapped within the same cavity but in the form of a complex that will not spontaneously collapse to the nitroso radical ion.

Finally, we would like to address a question that was raised by a reviewer of this manuscript: Why do the radical ions of **1** not fragment to yield **2**<sup>•</sup> and NO<sup>+</sup> or NO<sup>-</sup>, respectively? The reason is simply that the (gas-phase) ionization energy of NO• (9.26 eV) is ca. 2.5 eV higher than that of **2**<sup>•</sup> (cf. Table 1), so transferring an electron from NO• to **2**<sup>+</sup> is strongly endothermic, even in Ar, where this endothermicity may be attenuated by differential solvation effects. As the geometry of **2** does not depend

much on the presence or absence of an additional electron in its nonbonding HOMO (cf. Figure 8), we do not expect that the electron transfer between NO• and **2**<sup>+</sup> is associated with any barrier. Hence, NO<sup>+</sup> and **2**<sup>•</sup> are very unlikely to coexist for any length of time in the same matrix cavity. Similar arguments exclude the formation of NO<sup>-</sup> + **2**<sup>•</sup> from **1**<sup>•-</sup>: the electron affinity of NO• is close to zero, whereas that of **2**<sup>•</sup> is calculated to be over 1 eV. Even if the calculation is wrong by 0.5 eV (which it may be, because electron affinities are difficult to calculate accurately), electron transfer from **2**<sup>•</sup> to NO• will also be strongly endothermic. Thus, it comes as no surprise that we found no evidence for NO<sup>+</sup> or NO<sup>-</sup> in the IR spectra.

#### 4. Conclusions

*N*-Nitroso-*N,N*-diphenylamine **1** was exposed to X-irradiation in Ar matrices doped with CH<sub>2</sub>Cl<sub>2</sub> (an electron scavenger) or DABCO (a hole scavenger). Thereby, it was found that the radical cations and anions which result from these experiments mostly undergo spontaneous cleavage of the N–N bond to yield the diphenylnitrenium cation, **2**<sup>+</sup>, or the diphenylamide anion, **2**<sup>-</sup>, respectively, plus NO•. In the experiments with CH<sub>2</sub>Cl<sub>2</sub>, some evidence was found for a persistent radical cation, **1**<sup>•+</sup>, which could subsequently be photodecomposed to **2**<sup>+</sup> and NO•.

The most interesting results were obtained when **1** was first photodissociated to yield the diphenylaminyl radical, **2**<sup>•</sup>, which was subsequently subjected to ionization according to the above protocol. **2**<sup>+</sup>, **2**<sup>•</sup>, and **2**<sup>-</sup> were characterized by full UV–vis and IR spectra, which were unambiguously assigned on the basis of DFT calculations.

The results presented in this paper show that attachment or detachment of an electron to or from nitrosoamines significantly lowers the activation barrier for cleavage of the N–NO bond and release of the NO• radical.

The present method seems to be generally applicable for the generation of nitrenium cations R–N<sup>+</sup>–R and amide anions R–N<sup>-</sup>–R under the conditions of matrix isolation and in the absence of counterions, which allows their study by conventional spectroscopic methods. We plan to exploit this route to investigate derivatives that have not previously been studied, including *S*-nitrosothiols.

**Acknowledgment.** This work is part of project 200020-113268 of the Swiss National Science Foundation, the support of which is gratefully acknowledged. The work was also supported by a grant (No. 4/T09A/020/24) from the Polish Ministry of Science and Higher Education.

"A new Method for Generating Nitrenium Cations, Amide Anions and Aminyl Radicals under Stable Conditions"

by Krzysztof Piech, Thomas Bally,\* Adam Sikora, and Andrzej Marcinek\*.

#### SUPPORTING INFORMATION

\*\*\*\*\*

Full quote of the Gaussian Program (Reference 36):

M. J. Frisch, G. W. Trucks, H. B. Schlegel, G. E. Scuseria,  
M. A. Robb, J. R. Cheeseman, J. A. Montgomery, Jr., T. Vreven,  
K. N. Kudin, J. C. Burant, J. M. Millam, S. S. Iyengar, J. Tomasi,  
V. Barone, B. Mennucci, M. Cossi, G. Scalmani, N. Rega,  
G. A. Petersson, H. Nakatsuji, M. Hada, M. Ehara, K. Toyota,  
R. Fukuda, J. Hasegawa, M. Ishida, T. Nakajima, Y. Honda, O. Kitao,  
H. Nakai, M. Klene, X. Li, J. E. Knox, H. P. Hratchian, J. B. Cross,  
C. Adamo, J. Jaramillo, R. Gomperts, R. E. Stratmann, O. Yazyev,  
A. J. Austin, R. Cammi, C. Pomelli, J. W. Ochterski, P. Y. Ayala,  
K. Morokuma, G. A. Voth, P. Salvador, J. J. Dannenberg,  
V. G. Zakrzewski, S. Dapprich, A. D. Daniels, M. C. Strain,  
O. Farkas, D. K. Malick, A. D. Rabuck, K. Raghavachari,  
J. B. Foresman, J. V. Ortiz, Q. Cui, A. G. Baboul, S. Clifford,  
J. Cioslowski, B. B. Stefanov, G. Liu, A. Liashenko, P. Piskorz,  
I. Komaromi, R. L. Martin, D. J. Fox, T. Keith, M. A. Al-Laham,  
C. Y. Peng, A. Nanayakkara, M. Challacombe, P. M. W. Gill,  
B. Johnson, W. Chen, M. W. Wong, C. Gonzalez, and J. A. Pople,  
Gaussian 03, Rev. C-01, Gaussian, Inc., Wallingford CT, 2005.

Energies and geometries of all stationary points located  
and characterized in the course of the above study;

"r" denotes: radical

Note: All structures are optimized in vacuum, with energies  
in hartree.

1 - B3LYP/6-31G\*

Symmetry: c1

0 1  
6 -2.681174 -1.662609 -0.757227  
6 -3.796159 -1.079239 -0.153133  
6 -3.660066 0.147452 0.499828  
6 -2.423220 0.786536 0.561467  
6 -1.310205 0.202370 -0.058514  
6 -1.441909 -1.025635 -0.719396  
7 -0.046077 0.861008 -0.032826  
6 1.189244 0.133062 0.027508  
6 2.184234 0.348697 -0.930911  
6 3.380255 -0.363499 -0.850637  
6 3.583495 -1.289695 0.174431  
6 2.585802 -1.501354 1.128242  
6 1.390489 -0.787042 1.061478  
7 -0.094248 2.232960 -0.018041  
8 0.985118 2.792871 0.051866



1	-2.773680	-2.615664	-1.270727
1	-4.760689	-1.577631	-0.186696
1	-4.519103	0.607336	0.980620
1	-2.311957	1.731626	1.079493
1	-0.579963	-1.472678	-1.203231
1	2.021615	1.067848	-1.725530
1	4.153976	-0.194399	-1.594194
1	4.516303	-1.843802	0.230259
1	2.738399	-2.218647	1.929782
1	0.611708	-0.939001	1.802544

Electronic energy=	-647.945308
Sum of electronic and zero-point Energies=	-647.750164
Sum of electronic and thermal Enthalpies=	-647.737352
Sum of electronic and thermal Free Energies=	-647.789579
RCCSD	-645.970711

-----  
 1r+ - B3LYP/6-31G\*  
 Symmetry: c1

1	2			
6	-2.724830	-1.722253	-0.628382	
6	-3.835157	-1.010520	-0.142280	
6	-3.675677	0.285339	0.381461	
6	-2.427180	0.874591	0.428219	
6	-1.293909	0.156333	-0.057272	
6	-1.465306	-1.155240	-0.593540	
7	-0.049556	0.731196	-0.045427	
6	1.167927	0.055626	-0.013234	
6	2.239882	0.489229	-0.825597	
6	3.458024	-0.171688	-0.750102	
6	3.628677	-1.244012	0.136142	
6	2.569068	-1.669475	0.948978	
6	1.340984	-1.029870	0.881513	
7	-0.072780	2.362998	0.054319	
8	0.986695	2.810462	0.189457	
1	-2.857679	-2.712275	-1.052413	
1	-4.822525	-1.460295	-0.177477	
1	-4.536705	0.823810	0.763695	
1	-2.303613	1.860358	0.857582	
1	-0.610754	-1.676735	-1.009059	
1	2.098725	1.294619	-1.536910	
1	4.277340	0.141042	-1.389178	
1	4.588907	-1.747048	0.194628	
1	2.710243	-2.491426	1.643437	
1	0.523831	-1.323464	1.532351	

Electronic energy=	-647.669296
Sum of electronic and zero-point Energies=	-647.475470
Sum of electronic and thermal Enthalpies=	-647.462026
Sum of electronic and thermal Free Energies=	-647.515675
RCCSD	-645.693120

TDDFT B3LYP/6-31G\* excited state energies and transition moments:

1.3696 eV	905.25 nm	f=0.0293
1.4762 eV	839.88 nm	f=0.0197
1.5892 eV	780.17 nm	f=0.0133
1.9801 eV	626.16 nm	f=0.0572
2.2102 eV	560.96 nm	f=0.0167
2.5114 eV	493.68 nm	f=0.0398

2.9822 eV	415.75 nm	f=0.0134
3.0856 eV	401.82 nm	f=0.0049
3.1265 eV	396.56 nm	f=0.0435
3.3444 eV	370.72 nm	f=0.0035
3.4099 eV	363.60 nm	f=0.0081
3.5288 eV	351.35 nm	f=0.0103
3.6919 eV	335.82 nm	f=0.0058
3.8287 eV	323.82 nm	f=0.0081
3.9278 eV	315.66 nm	f=0.0616
4.0640 eV	305.08 nm	f=0.0019
4.1245 eV	300.61 nm	f=0.0640
4.1665 eV	297.57 nm	f=0.0478

1+....NOr (the most stable complex) - B3LYP/6-31G\*  
Symmetry: c1

1	2		
6	-2.155842	-1.479764	-0.799803
6	-3.156950	-1.344715	0.182263
6	-2.947646	-0.550927	1.321505
6	-1.743408	0.109006	1.482611
6	-0.672977	-0.090817	0.549110
6	-0.929545	-0.867288	-0.632653
7	0.475269	0.533045	0.855910
6	3.400865	-1.227307	-0.575881
6	4.319590	-0.161404	-0.523626
6	3.954427	1.083102	0.015063
6	2.674509	1.266583	0.501478
6	1.697925	0.224547	0.385409
6	2.104452	-1.049176	-0.136420
1	-2.359024	-2.052795	-1.699168
1	-4.112082	-1.842432	0.041998
1	-3.736605	-0.438698	2.058234
1	-1.545037	0.738806	2.343603
1	-0.180154	-0.916030	-1.414843
1	3.723042	-2.197385	-0.940822
1	5.336053	-0.316971	-0.873309
1	4.682211	1.885979	0.070300
1	2.356812	2.205851	0.941504
1	1.418022	-1.887863	-0.102879
8	-3.694065	1.501866	-1.234604
7	-2.661428	1.943464	-1.021927

Electronic energy=	-647.658910
Sum of electronic and zero-point Energies=	-647.466750
Sum of electronic and thermal Enthalpies=	-647.452044
Sum of electronic and thermal Free Energies=	-647.510598

1r- - B3LYP/6-31G\*  
Symmetry: c1

-1	1		
6	3.017104	-1.704092	0.160582
6	4.044677	-0.780929	-0.055657
6	3.703675	0.578079	-0.110921
6	2.389168	0.999298	0.035083
6	1.318596	0.078140	0.235794
6	1.692069	-1.298491	0.299018
7	0.068045	0.575022	0.465949

6	-1.087699	-0.114406	0.244847
6	-2.253992	0.319366	0.938985
6	-3.495443	-0.272535	0.735408
6	-3.652610	-1.324916	-0.173962
6	-2.527472	-1.755646	-0.888260
6	-1.280926	-1.169883	-0.696787
7	-0.287187	2.629275	-0.595187
8	-1.420626	2.927130	-0.429405
1	3.251122	-2.767357	0.228283
1	5.076598	-1.106368	-0.170079
1	4.483358	1.324053	-0.268864
1	2.137413	2.054223	0.001217
1	0.925047	-2.042052	0.493613
1	-2.134914	1.132231	1.649331
1	-4.356434	0.090839	1.296718
1	-4.623393	-1.792009	-0.327166
1	-2.627563	-2.559810	-1.618170
1	-0.435127	-1.504780	-1.289758

Electronic energy=	-647.969712
Sum of electronic and zero-point Energies=	-647.779867
Sum of electronic and thermal Enthalpies=	-647.765649
Sum of electronic and thermal Free Energies=	-647.821918
RCCSD	-645.974974

TDDFT B3LYP/6-31G\* excited state energies and transition moments:

0.7300 eV	1698.43 nm	f=0.0000
2.0433 eV	606.79 nm	f=0.0058
2.8061 eV	441.83 nm	f=0.0171
2.8899 eV	429.02 nm	f=0.0097
3.0613 eV	405.00 nm	f=0.0004
3.1560 eV	392.85 nm	f=0.0000
3.3065 eV	374.97 nm	f=0.0153
3.3660 eV	368.35 nm	f=0.0056
3.6308 eV	341.48 nm	f=0.0216
4.0074 eV	309.39 nm	f=0.3744
4.0465 eV	306.40 nm	f=0.0038

1+ - B3LYP/6-31G\*  
Symmetry: c2

1	1		
6	0.383305	2.765720	-1.385985
6	-0.117237	3.804535	-0.575152
6	-0.520532	3.565886	0.748748
6	-0.424191	2.289677	1.268040
6	0.000000	1.199416	0.437587
6	0.440854	1.475616	-0.901827
7	0.000000	0.000000	1.041177
6	-0.383305	-2.765720	-1.385985
6	0.117237	-3.804535	-0.575152
6	0.520532	-3.565886	0.748748
6	0.424191	-2.289677	1.268040
6	0.000000	-1.199416	0.437587
6	-0.440854	-1.475616	-0.901827
1	0.746292	2.990637	-2.383695
1	-0.156626	4.814884	-0.972238
1	-0.879437	4.384130	1.364157
1	-0.707185	2.061179	2.290073
1	0.898493	0.688808	-1.490883

1	-0.746292	-2.990637	-2.383695
1	0.156626	-4.814884	-0.972238
1	0.879437	-4.384130	1.364157
1	0.707185	-2.061179	2.290073
1	-0.898493	-0.688808	-1.490883

Electronic energy=	-517.766161
Sum of electronic and zero-point Energies=	-517.579045
Sum of electronic and thermal Enthalpies=	-517.568262
Sum of electronic and thermal Free Energies=	-517.614473
RCCSD	-516.120174

TDDFT B3LYP/6-31G\* excited state energies and transition moments:

1.9791 eV	626.47 nm	f=0.1008
2.4723 eV	501.50 nm	f=0.0119
2.5265 eV	490.74 nm	f=0.0034
3.4701 eV	357.29 nm	f=0.6377
4.2533 eV	291.50 nm	f=0.0056
4.6504 eV	266.61 nm	f=0.0032
4.8868 eV	253.71 nm	f=0.0027
4.9086 eV	252.58 nm	f=0.0000
5.2738 eV	235.09 nm	f=0.0034
5.4524 eV	227.39 nm	f=0.0126

1r - B3LYP/6-31G\*  
Symmetry: c2

0 2			
6	0.546664	2.728404	-1.345575
6	0.005429	3.802252	-0.629436
6	-0.516655	3.586592	0.653187
6	-0.499438	2.317066	1.209853
6	0.000000	1.202602	0.481835
6	0.542133	1.445732	-0.811629
7	0.000000	0.000000	1.133080
6	-0.546664	-2.728404	-1.345575
6	-0.005429	-3.802252	-0.629436
6	0.516655	-3.586592	0.653187
6	0.499438	-2.317066	1.209853
6	0.000000	-1.202602	0.481835
6	-0.542133	-1.445732	-0.811629
1	0.982727	2.897511	-2.326873
1	0.008165	4.800415	-1.058129
1	-0.923434	4.419254	1.220817
1	-0.883475	2.131705	2.208117
1	0.999069	0.628347	-1.359125
1	-0.982727	-2.897511	-2.326873
1	-0.008165	-4.800415	-1.058129
1	0.923434	-4.419254	1.220817
1	0.883475	-2.131705	2.208117
1	-0.999069	-0.628347	-1.359125

Electronic energy=	-518.014346
Sum of electronic and zero-point Energies=	-517.829093
Sum of electronic and thermal Enthalpies=	-517.818280
Sum of electronic and thermal Free Energies=	-517.865258
RCCSD	-516.365681

TDDFT B3LYP/6-31G\* excited state energies and transition moments:

1.6530 eV	750.07 nm	f=0.0444
-----------	-----------	----------



2.8265 eV	438.65 nm	f=0.0038
2.8877 eV	429.35 nm	f=0.0014
3.1149 eV	398.03 nm	f=0.0366
3.6813 eV	336.80 nm	f=0.0021
4.0053 eV	309.55 nm	f=0.0493
4.1361 eV	299.76 nm	f=0.0079
4.1372 eV	299.68 nm	f=0.3606
4.2057 eV	294.80 nm	f=0.0040
4.4555 eV	278.27 nm	f=0.1133

---

1- - B3LYP/6-31G\*  
Symmetry: c1

-1	1		
6	0.534702	2.781771	-1.345136
6	0.059067	3.873248	-0.609271
6	-0.435004	3.624372	0.680688
6	-0.460075	2.340698	1.205055
6	0.000000	1.199286	0.473396
6	0.508138	1.487151	-0.834893
7	0.000000	0.000000	1.108682
6	-0.534702	-2.781771	-1.345136
6	-0.059067	-3.873248	-0.609271
6	0.435004	-3.624372	0.680688
6	0.460075	-2.340698	1.205055
6	0.000000	-1.199286	0.473396
6	-0.508138	-1.487151	-0.834893
1	0.943384	2.943586	-2.344087
1	0.076865	4.880272	-1.020921
1	-0.806059	4.452694	1.286132
1	-0.835775	2.157498	2.209573
1	0.912921	0.673874	-1.430117
1	-0.943384	-2.943586	-2.344087
1	-0.076865	-4.880272	-1.020921
1	0.806059	-4.452694	1.286132
1	0.835775	-2.157498	2.209573
1	-0.912921	-0.673874	-1.430117

Electronic energy=	-518.067063
Sum of electronic and zero-point Energies=	-517.883521
Sum of electronic and thermal Enthalpies=	-517.872631
Sum of electronic and thermal Free Energies=	-517.919038
RCCSD	-516.404724

TDDFT B3LYP/6-31G\* excited state energies and transition moments:

3.4588 eV	358.46 nm	f=0.0184
3.5788 eV	346.44 nm	f=0.0192
3.8360 eV	323.21 nm	f=0.6337
4.5480 eV	272.61 nm	f=0.0017
4.7604 eV	260.45 nm	f=0.0131
4.8024 eV	258.17 nm	f=0.0092
5.3217 eV	232.98 nm	f=0.0160
5.3579 eV	231.40 nm	f=0.0004
5.4963 eV	225.58 nm	f=0.0060
5.9163 eV	209.57 nm	f=0.0903

---

NOr - B3LYP/6-31G\*  
Symmetry: c\*v

```
0 2
7      0.000000      0.000000      -0.617973
8      0.000000      0.000000      0.540727
```

```
Electronic energy= -129.888156
Sum of electronic and zero-point Energies= -129.883620
Sum of electronic and thermal Enthalpies= -129.880315
Sum of electronic and thermal Free Energies= -129.903626
RCCSD -129.563051
-----
```

Attachment converted: IMac G4 HD:krzysztof.piech.vcf (TEXT/MSWD) (01CCFD22)